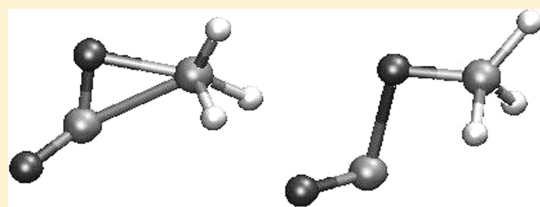


Thermal Decomposition of Condensed-Phase Nitromethane from Molecular Dynamics from ReaxFF Reactive Dynamics

Si-ping Han,^{†,‡} Adri C. T. van Duin,[‡] William A. Goddard, III,[‡] and Alejandro Strachan^{*,§}[†]Theoretical Division, Los Alamos National Laboratory, Los Alamos, New Mexico 87545, United States[‡]Materials and Process Simulation Center, Beckman Institute (139-74), California Institute of Technology, Pasadena, California 91125, United States[§]School of Materials Engineering, Purdue University, West Lafayette, Indiana 47907, United States

ABSTRACT: We studied the thermal decomposition and subsequent reaction of the energetic material nitromethane (CH_3NO_2) using molecular dynamics with ReaxFF, a first principles-based reactive force field. We characterize the chemistry of liquid and solid nitromethane at high temperatures (2000–3000 K) and density 1.97 g/cm^3 for times up to 200 ps. At $T = 3000 \text{ K}$ the first reaction in the decomposition of nitromethane is an intermolecular proton transfer leading to CH_3NOOH and CH_2NO_2 . For lower temperatures ($T = 2500$ and 2000 K) the first reaction during decomposition is often an isomerization reaction involving the scission of the C–N bond the formation of a C–O bond to form methyl nitrate (CH_3ONO). Also at very early times we observe intramolecular proton transfer events. The main product of these reactions is H_2O which starts forming following those initiation steps. The appearance of H_2O marks the beginning of the exothermic chemistry. Recent quantum-mechanics-based molecular dynamics simulations on the chemical reactions and time scales for decomposition of a crystalline sample heated to $T = 3000 \text{ K}$ for a few picoseconds are in excellent agreement with our results, providing an important, direct validation of ReaxFF.



INTRODUCTION

A molecular-level understanding of condensed-phase chemistry is among the central challenges of the atomistic modeling community; such a fundamental understanding is critical in many areas including materials for the energy sector and high-energy density materials. *Ab initio* quantum mechanical (QM) methods to obtain first principles predictions of the mechanisms, barriers, and rates of unimolecular (see for example ref 1) and bimolecular² reactions have dramatically improved our understanding of chemical reactions relevant to many fields including energetic materials^{1,2} and catalysis.³ Such QM studies are computationally intensive and are typically limited to relatively small systems and short times (roughly ~ 100 atoms for a few picoseconds). Furthermore, QM studies usually focus on gas phase phenomena; thus, pressure effects and multimolecular reactions can only be taken into account approximately. An exception are recent QM based molecular dynamics (MD) studies of high temperature decomposition of energetic materials^{4–6} that follow condensed-phase dynamics of the system in full atomistic detail. The computational cost of QM limits most simulations to small systems over the course of a few picoseconds. A recently developed method allows coupling of a small QM region with a continuum description of a much larger system.^{7,8} This illuminates some aspects of the physics and chemistry, but full scale molecular dynamics on larger systems are still needed.

To achieve longer simulation times in larger systems, it is possible to replace the QM description with a force field (FF) that describes atomic interactions in a computationally efficient

manner. This has allowed MD simulations for up to microseconds and is routinely used for tens of nanoseconds. A severe limitation of this approach has been that such classical FFs have been incapable of describing correctly the breaking and forming of covalent bonds, that is, reaction chemistry. Over the past few years we have been developing a new generation of FF (denoted ReaxFF) aimed at accurately describing, in a computationally efficient manner, the chemistry of a wide range of materials. ReaxFF uses general relationships to describe how charge flows between atoms and how the valence energies depend on geometry. Thus, the valence energies are described in terms of bond orders that are uniquely determined from the atomic positions (no predetermined assignment of bond types), and the parameters used in ReaxFF are obtained from QM calculations on structures and reactions for a large set of systems. ReaxFF has now been used successfully for a number of allowed and forbidden reactions of hydrocarbons,⁹ oxidation of metals such as Si, Al, and Pt,^{10,11} and for shock¹² and thermal¹³ induced decomposition the energetic material RDX [cyclic $(\text{CH}_2\text{N}(\text{NO}_2))_3$]. The use of this type of force field to predict complex processes in real materials (often under high temperatures and pressure) is growing at a rapid pace, and there is a serious need for a critical assessment of their accuracy. Among the many possible applications of ReaxFF, the decomposition

Received: October 31, 2010

Revised: March 28, 2011

Published: May 04, 2011

and reaction of energetic materials are among the most challenging ones due to the complex chemistry involved and the extreme conditions of temperature and pressure involved.

In this paper we use ReaxFF with MD to study the thermal-induced decomposition and subsequent reactions of the energetic material nitromethane (CH_3NO_2) at high temperatures (from 2000 to 3000 K) and high density $\rho = 1.97$ (normal density is 1.13 g/cm^3) for times up to 200 ps. We report here the thermal decomposition of liquid and crystalline samples of nitromethane that are instantaneously heated to the desired final temperature. Reactive MD simulations provide a molecular-level description of the chemistry and mechanical processes in energetic materials making no assumptions or simplifications other than those intrinsic to the force field description of the interactions, the fact that we use classical mechanics to describe atomic dynamics, and the size of the simulation cell. Our simulations show that the first chemical events involve an intramolecular proton transfer leading to CH_2NO_2 and CH_3NOOH or an isomerization reaction leading to CH_3ONO . This is the first time that such isomerization has been observed in condensed-phase simulations. We also find intramolecular proton transfer at early times (within about a picosecond for $T = 3000 \text{ K}$). After these initial events, N–O bond breaking leads to the formation of H_2O and the initiation of the exothermic chemistry. At this point the potential energy decreases dramatically as the pressure increases while the average molecular weight of the system decreases. We choose nitromethane due to the extensive experimental characterization of this material and also to compare the ReaxFF results with recent work by Manaa and collaborators who used QM-based MD to heat a crystal to 3000 K for time scales of around 1 ps. We find very good agreement between our ReaxFF simulations and QM-based ones both regarding nature of the initial chemical reactions as well as their time scales; this provides an important validation of the ReaxFF description of reactive atomic interactions of CHNO materials.

After a brief description of relevant previous work (section II), in section III we describe ReaxFF and our MD simulations. In section IV we present the energetics of decomposition and pressures involved. Section V describes the key chemical events, and section VI focuses on the atomic diffusivity of reactants and products. Finally, section VII draws conclusions.

■ BACKGROUND

Nitromethane is one of the most extensively studied energetic materials both experimentally and theoretically. It is generally agreed that under low pressure conditions the first reaction in the decomposition of NM is the homolytic breaking of the C–N bond; this reaction, having a positive volume of activation, does not play an important role under high pressures.

Several observations (see for example ref 14) indicate that the presence of the aci ion form of NM (CH_2NO_2) has an important effect in accelerating the chemical reactions. Engelke and collaborators showed that the aci ion form is the only new species in base-sensitized NM.¹⁵ Recent infrared spectroscopy experiments show that intramolecular proton transfer leading to the aci form is among the first events in the room temperature decomposition of NM at high pressures.¹⁶ In addition, the decrease of reaction time with increasing pressure¹⁷ has also been attributed to the increased population of the aci ion with pressure.¹⁸ Time-of-flight mass spectroscopy studies of the reaction zone of detonating

base-sensitized NM show species resulting from condensation reactions involving two or more NM molecules.

From a theoretical point of view the recent development of partial bond-order-based reactive force fields opens the opportunity to characterize the chemistry of energetic materials under conditions approaching those in experiments.

Developing a fundamental understanding of energetic materials requires characterizing complex, inter-related mechanical and chemical processes at extreme conditions of temperature and pressure and is essential for the development of physics-based, predictive models of energetic materials that can aid the design of safer materials with improved properties. A molecular-level characterization of the processes of decomposition and reaction of condensed-phase energetic materials is a very challenging problem, and force fields for MD simulations capable of describing chemical reactions^{9,19} are playing an increasingly important role. Large-scale MD with bond-order-dependent reactive potentials that exhibit simple exothermic chemistry²⁰ have provided very valuable information about generic properties of energetic materials such as the equilibrium structure of steady state detonation waves,^{20,21} role of defects,^{22,23} the existence of a failure diameter,²⁴ and desensitization.²⁵ The recent development of reactive potentials^{9,19} that can describe the chemistry of real materials (including HE) has enabled the characterization of shock-induced chemistry¹² and thermal decomposition in a wide temperature and pressure range.¹² However, before quantitative conclusions on real materials can be drawn from these simulations a critical assessment of their accuracy needs to be performed.

■ COMPUTATIONAL METHODS

Reactive Force Field ReaxFF. The key concepts that enable ReaxFF to describe complex chemical reactions are the use of (1) environment dependent atomic charges (updated at every step during the dynamics) to describe electrostatics, (2) partial bond orders (a many body contribution based purely on atomic positions) to describe covalent interactions, and (3) two-body terms (between all atoms) to account for London dispersion attraction and short-range Pauli repulsion (often denoted as van der Waals terms).

We have recently described the energy expression of ReaxFF and the training set used to parametrize the potential for RDX simulations. This FF has been recently improved with the addition of QM results on chemical reactions involving nitromethane and vibrational information (frequencies and modes) of small molecules to the training set. The details of the new chemical reactions used for the ReaxFF parametrization were published in ref 26.

Molecular Dynamics Simulations. We use ReaxFF with MD to simulate the decomposition of liquid and crystalline samples of nitromethane at temperatures from $T = 2000 \text{ K}$ to $T = 3000 \text{ K}$ and density $\rho = 1.97 \text{ g/cm}^3$ (corresponding to a volume 75% of the zero pressure volume of the crystal). The crystalline samples contain 16 molecules and were obtained by replicating the unit cell two times in the y and z directions followed by a thermalization at $T = 10 \text{ K}$. This same structure was used in ref 4 with QM-based MD to characterize the initial chemistry of nitromethane at $T = 3000 \text{ K}$. The liquid samples contain 32 nitromethane molecules and are built using the nonreactive force field DREIDING;²⁷ we perform high temperature ($T = 500 \text{ K}$) MD simulations starting with a low density simulation cell (where the molecules have very high mobility) and compress it until the

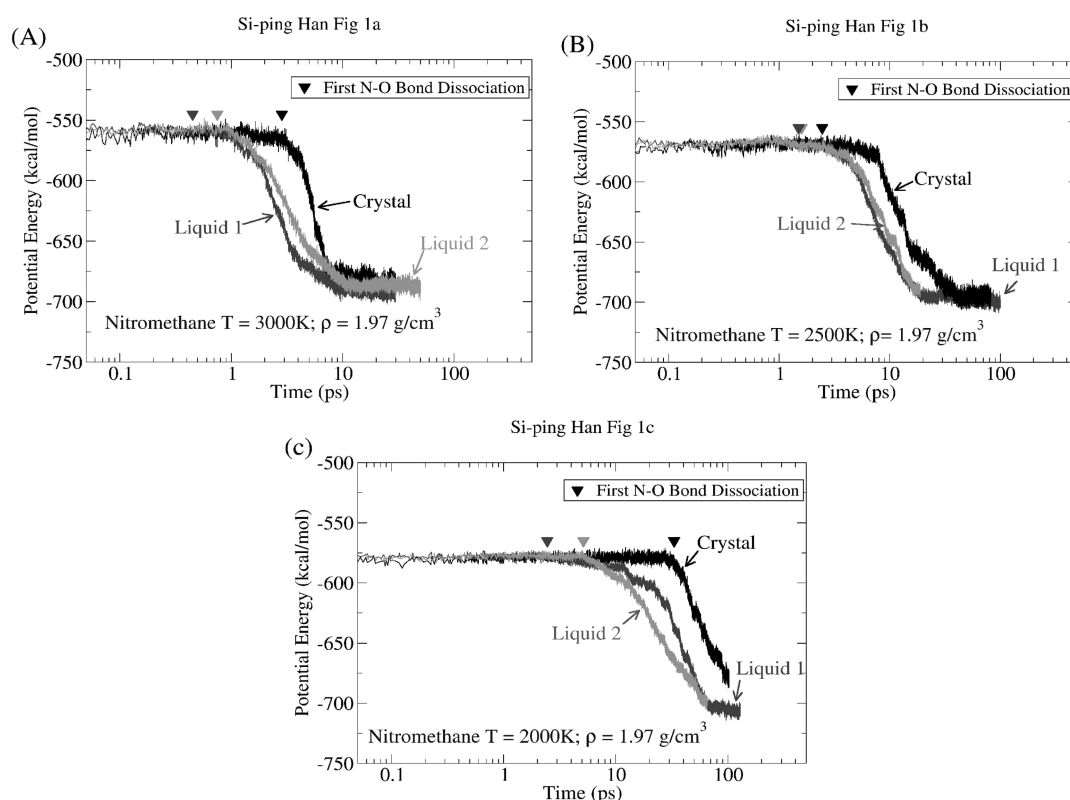


Figure 1. Time evolution of the potential energy (in kcal/mol per nitromethane molecule) for temperatures 3000 K (a), 2500 K (b), and 2000 K (c). Triangles show the time corresponding to the first N–O bond breaking event.

desired density (1.97 g/cm^3) is achieved. This structure is then quenched with isothermal isochoric MD using the ReaxFF potential at $T = 10 \text{ K}$ to obtain the first liquid sample (denoted liquid 1). We then run 40 ps NVT MD at $T = 500 \text{ K}$ with ReaxFF and rethermalize the resulting structure at $T = 10 \text{ K}$ to obtain a second, uncorrelated, liquid structure (liquid 2).

We simulate the decomposition of all three structures using isothermal isochoric MD (NVT ensemble) using a Berendsen thermostat with a coupling constant of 200 fs. The initial velocities are chosen from the Maxwell–Boltzmann distribution with temperature two times the desired temperature. Since the initial potential energy is close to the ground state, the kinetic energy decreases to roughly half its initial value very quickly (few tens of femtoseconds). We also perform an annealing simulation of a crystalline sample at $\rho = 2.20 \text{ g/cm}^3$. This sample was heated from $T = 1000$ to 4000 K to compare the resulting pressure profile with QM results reported in ref 4.

INTERNAL ENERGY AND PRESSURE EVOLUTION DURING DECOMPOSITION

In Figure 1 we show the time evolution of the potential energy for liquid and crystalline nitromethane. Figure 1a,b,c corresponds to $T = 3000 \text{ K}$, $T = 2500 \text{ K}$, and $T = 2000 \text{ K}$, respectively. After a temperature dependent induction time during which the energy remains essentially constant and the first chemical reactions occur (as will be discussed in the next section) the potential energy decreases abruptly as exothermic reactions begin.

In all cases shown in Figure 1 the liquid samples exhibit faster chemistry than crystalline ones; however, the time scales of decomposition in our simulations are not well converged with

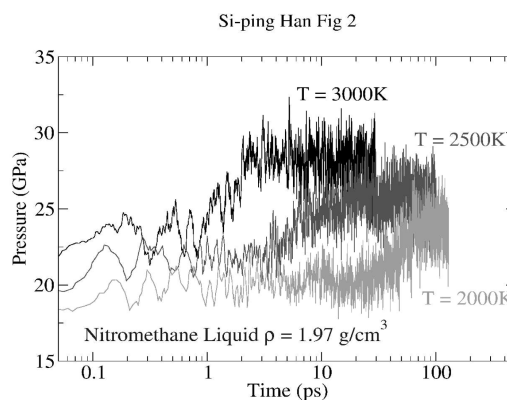


Figure 2. Time evolution of the pressure for the liquid structure at three temperatures: $T = 3000 \text{ K}$, $T = 2500 \text{ K}$, and $T = 2000 \text{ K}$.

respect to simulation size. Simulation cells large enough to allow multiple independent initiation events are necessary to obtain accurate decomposition time scales. We are currently assessing the cell size dependency of reaction times.

In Figure 2 we show the time evolution of the pressure during the reaction of the liquid 1 sample at temperatures $T = 2000$, 2500 , and 3000 K . Before the chemical reactions occur the pressures range from $\sim 18 \text{ GPa}$ at $T = 2000$ to 22 GPa at $T = 3000 \text{ K}$. As the reactions proceed and the number of molecules increases, the pressures increase by $\sim 15\%$; the final pressures range from ~ 23 to $\sim 29 \text{ GPa}$.

In order to validate the accuracy of the ReaxFF description of mechanical properties under such large compression and

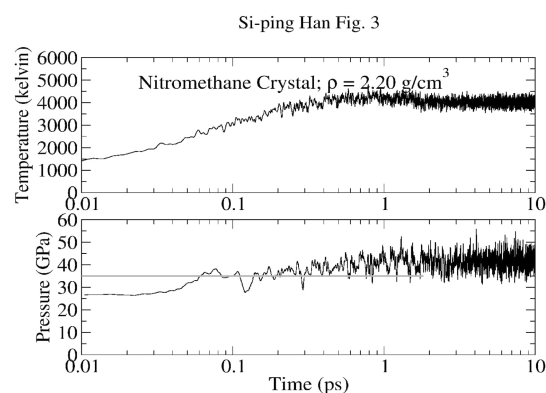


Figure 3. Time evolution of the temperature (a) and pressure (b) of crystalline nitromethane during a fast annealing from $T = 1000$ K to $T = 4000$ K. QM-based MD⁴ at $T = 1000$ K lead to a pressure of 25 GPa in good agreement with our results (24.7 GPa). When the temperature is increased to 4000 K (in a ~ 0.6 ps run) the pressure rises to 35 GPa, also in agreement with our results. Note that for longer times our simulations predict a further increase in the pressure.

temperature we performed a simulation at a higher density ($\rho = 2.2$ g/cm³) since pressures from QM-based MD simulations are available for this density.⁴ As in ref 4 we performed a short simulation (0.2 ps) at $T = 1000$ K and then quickly heated the system up to $T = 4000$ K. Using ReaxFF we obtain a pressure $P = 24.70$ GPa for the $T = 1000$ K simulation (averaged over the last 100 fs of the simulation); this value is in excellent agreement with the reported QM result (25 GPa). In Figure 3 we show the temperature (a) and pressure (b) evolution during the annealing run that takes the system from $T = 1000$ K to $T = 4000$ K. The QM results indicate that the pressure rises and stabilizes at about 35 GPa (the total length of the run was 0.6 ps); this value is indicated as a horizontal line in Figure 3b. Again the ReaxFF results are in very good agreement with the QM results. Note that for times longer than the QM run the pressure increases further to about 40 GPa. These results indicate that ReaxFF provides a very accurate description of the equation of state of nitromethane at high pressures and temperatures.

■ DECOMPOSITION AND REACTION CHEMISTRY

The reactive MD simulations in this paper provide a very detailed, molecular-level description of the decomposition and reaction of nitromethane under various conditions. Such information should allow one to extract valuable information about the complex chemistry involved, including uni- and multimolecular reactions, catalytic steps, etc.

In Table 1 we show the times corresponding to the first bond breaking and formation for a variety of bonds and for all our simulations. In each case the first bond breaking event is marked with an asterisk. Our simulations show that the first reaction during decomposition is either an intermolecular proton transfer leading to CH_2NO_2 and CH_3NOOH , or an isomerization reaction leading to methyl nitrite (CH_3ONO). The proton transfer involves breaking a C–H bond and forming a new bond between the proton and an oxygen in a nearby molecule (notice the correlation between C–H breaking and O–H formation times in Table 1). The partial charge of the H atom transferred during the reaction is approximately $+0.2$ e, indicating that under such condensed phase conditions the reaction is not ideally ionic.

Table 1. Times (in ps) of First Bond Breaking, Bond Formation, and Intramolecular Proton Transfer for the Various Simulations^a

configuration	bond breaking			bond formation		intramolecular proton transfer
	C–H	C–N	N–O	O–H	C–O	
crystal ($T = 3000$ K)	0.1*	2.8	1.6	0.1	0.1	1.38
liquid 1 ($T = 3000$ K)	0.05*	0.5	0.4	0.05	0.1	1.13
liquid 2 ($T = 3000$ K)	0.3*	0.7	0.7	0.3	0.5	1.17
crystal ($T = 2500$ K)	2.4	0.7*	2.4	2.4	1.0	
liquid 1 ($T = 2500$ K)	0.9	0.6*	1.5	0.9	0.6	
liquid 2 ($T = 2500$ K)	0.5*	2.2	1.5	0.4	0.7	0.45
crystal ($T = 2000$ K)	28.0	26.4*	33.1	28.0	26.5	51.95
liquid 1 ($T = 2000$ K)	2.0*	7.4	2.4	2.0	2.0	37.42
liquid 2 ($T = 2000$ K)	4.6	0.7*	5.1	4.6	0.9	

^a Asterisks mark first bond breaking events.

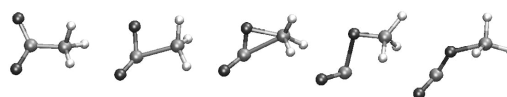


Figure 4. Snapshots of isomerization reaction leading to methyl nitrate obtained from the MD simulation of liquid 1 at $T = 2000$ K. The central snapshot corresponds roughly to the transition state whose structure is in good agreement with recent *ab initio* results.²⁸

This is in agreement with Mulliken charges in QM-based simulations of Manaa et al.;⁴ they find a charge of about $+0.3e$ for the same atom. In Figure 4 we show five snapshots of the isomerization reaction obtained from our MD simulation of the liquid 1 structure at $T = 2500$ K; the time elapsed between the second and the fourth snapshots is 20 fs. The central structure depicts roughly the transition state. It is worth emphasizing that, while a single molecule is shown in Figure 4, our simulation resolves in full atomistic detail the dynamics of 32 molecules in the condensed phase at high density; all multimolecular effects are resolved exactly in our simulation. The C–N and C–O bond distances corresponding to the condensed phase transition state we observe with ReaxFF are 1.89 and 1.60 Å, respectively. There has been some controversy in the literature regarding the structure of the transition state between nitromethane and methyl nitrate, see for example, ref 28. Some authors have predicted a loose transition state (with C–N and C–O bond distances longer than 3 Å)²⁹ while others predict a tight transition state with bond distances around 2 Å. Our MD simulations predict a tight transition state in agreement with recent *ab initio* results;²⁸ we did not observe an *initial* reaction matching the loose transition state.²⁹

Although more simulations would be necessary to obtain better statistics, our simulations indicate that the higher-frequency, higher-activation energy C–H breaking process is more likely to be the initial reaction at high temperatures whereas the lower-frequency lower-activation energy isomerization reaction leading to methyl nitrate tends to be the initial reaction at low temperatures. This is in qualitative agreement with ref 29.

All the first chemical events shown in Table 1 happen during the induction time where the potential energy is approximately constant; triangles in Figure 1 mark the time of the first N–O

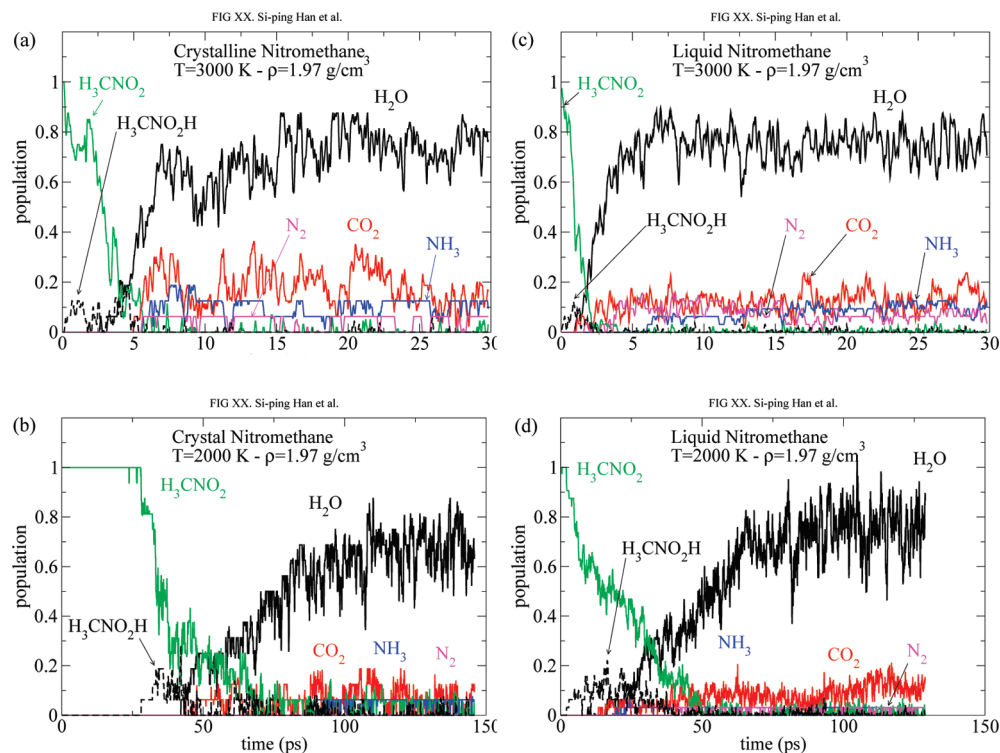


Figure 5. Time evolution of nitromethane (green lines), several important products [H_2O (black), CO_2 (red), N_2 (magenta), and NH_3 (blue)], and the intermediate H_3CNOOH (dashed lines) for the liquid and crystalline structures at $T = 3000 \text{ K}$ and $T = 2000 \text{ K}$. Populations are given per nitromethane molecule.

bond breaking process. We see that the exothermic chemistry starts not long after the first N–O bond breaking.

Using QM-based MD, Manaa and collaborators⁴ studied the decomposition of solid nitromethane heated to 3000 K and found that the first reaction was an intermolecular proton transfer. The resulting time scales for this first reaction were 0.059, 0.780, and 0.785 ps in three independent simulations. Our results (0.05, 0.1, and 0.3 ps also in three independent simulations) are in quantitative agreement with the QM results; this provides an important direct validation of ReaxFF against a first principles, QM-based description of the atomic interactions.

In many simulations we observe intramolecular proton transfer from the methyl to the nitro group leading to the aci acid form of nitromethane CH_2NOOH ; Table 1 shows the corresponding times for this isomerization reaction. This result is also in agreement with QM results.⁴

For the crystal at $T = 3000 \text{ K}$, we find that the very first water produced contains a hydroxyl group from the nitrogen end of a $\text{COH}-\text{NOOH}$ and a proton from a formaldehyde. The hydroxyl group is formed by intramolecular proton transfer from the CH_3 end of a nitromethane to the NO_2 end of another one. The carbon end of that molecule subsequently undergoes several reactions, resulting in $\text{COH}-\text{NOOH}$. The formaldehyde is created through several steps beginning with the dissociation of a CH_3 group from a nitromethane. Subsequently, this group lost a hydrogen and then gained an oxygen by inducing a N–O bond to break in a nitromethane remnant. The resulting formaldehyde then contributed one of its protons to form water.

In Figure 5 we show the time evolution of the population of nitromethane as well as several important products (H_2O , CO_2 , N_2 , and NH_3) and the intermediate (H_3CNOOH) for both

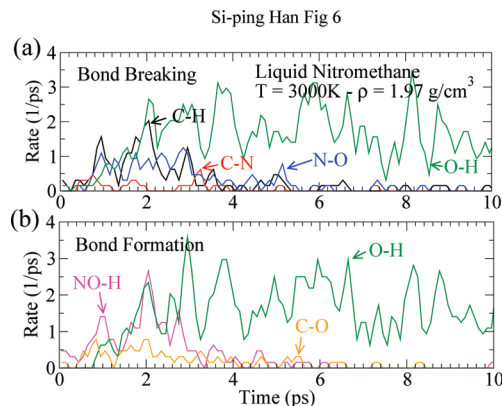


Figure 6. Bond breaking and forming rates for the liquid 1 structure at $T = 2000$ and $T = 3000 \text{ K}$.

liquid and crystalline structures and two temperatures. As already mentioned the formation of CH_3NOOH via a proton transfer is the first reaction that appears in the populations plot. The formation of H_2O (the main product) occurs after most of the original nitromethane molecules have undergone the initiation reactions. The final population of H_2O is not very sensitive to temperature; we find about 0.8 H_2O molecules per nitromethane. Other important products are N_2 , CO_2 , and NH_3 . As expected the population of these small molecules is larger at $T = 3000 \text{ K}$ than at $T = 2000 \text{ K}$; in particular, we find essentially no N_2 molecules at $T = 2000 \text{ K}$.

In Figure 6 we plot the rate of bond breaking and formation (number of bonds broken or formed per unit time per nitromethane molecule) for various key pairs of atoms. As already

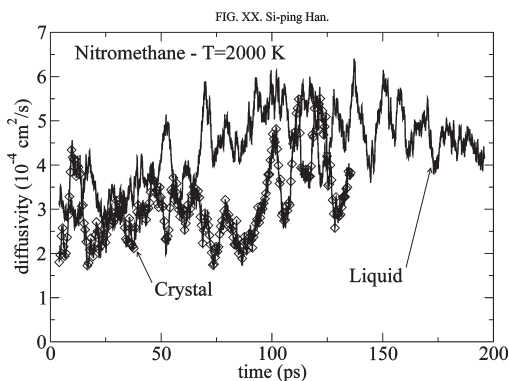


Figure 7. Time evolution of the diffusion constant of O atoms for liquid and crystalline nitromethane at $T = 2000$ K.

mentioned the initial reactions involve breaking C–H and C–N bonds and forming O–H and C–O ones. We can see from Figure 6 the time scales of the various reactions. For long times we find the main events are O–H bond breaking and forming (with equal rates). This is because H_2O is the main product and the molecules at this high temperatures undergo frequent chemical reactions under dynamical equilibrium.

Besides the small molecules reported above, decomposition leads to several larger molecular fragments. These molecules contain between $\sim 70\%$ and $\sim 40\%$ of the total carbon and nitrogen of the system, but we find no sign of initial carbon clustering within the relatively short time of our simulations; the largest number of C atoms observed in a molecule is three. This is consistent with experimental observations.³⁰

■ ATOMIC DIFFUSION DURING REACTIONS

Diffusion of atomic species during the decomposition and reaction of energetic materials is an important phenomenon that governs molecular intermixing and plays an important role in the degree of completion of the chemical reactions during detonation or combustion as well as in the process of carbon clustering. The formation of condensed-phase aggregates composed mostly of C atoms is most important since it governs the balance between CO and CO_2 (see for example ref 12) which, in turn, can dramatically affect the exothermicity of the HE material.

Atomic diffusivity is not easily accessible experimentally under the extreme conditions characteristic of HE materials, making the estimates from MD very valuable. The diffusion constant (D) can be defined from the time evolution of the atomic mean square displacement $[\Delta r^2(t)]$

$$\Delta r^2(t) = \lim_{T \rightarrow \infty} \frac{1}{T} \int_0^T dt \frac{1}{N} \sum_i [(r(t' + t) - r(t'))^2] = 6Dt \quad (1)$$

where N is the number of atoms involved.

In describing diffusion it is important to wait sufficiently long times such that Δr^2 becomes proportional to time (Fickian behavior). This is not possible in our case since the decomposition occurs in relatively short times. Consequently, we define an effective, local in time, diffusion constant. We obtain the effective diffusion constants from our MD simulations by averaging over 8 ps.

In Figure 7 we show the time evolution of the diffusion constant of oxygen atoms at $T = 2000$ K both for liquid and crystalline samples. Despite the large fluctuations of the data we

find the initial oxygen diffusivity in the liquid samples is larger than that in the solid one. This is consistent with our observation of faster initial decomposition of the liquid samples, see Figures 1 and 5. The decomposition and subsequent chemical reactions lead to a decrease in the molecular size of the system and consequently an increase in diffusivity: our simulations show an increase of approximately 50%. Finally, as the products are formed information about the initial structure of the material (crystalline or liquid) is lost and both classes of samples exhibit similar diffusivities.

■ DISCUSSION: ReaxFF VALIDATION

Our results for the crystalline sample at $T = 3000$ K are in good agreement with recent QM-based MD simulations⁴ not only regarding the initial chemical reactions of the decomposition and the associated time scales but also in the equation of state of NM up to very high pressures. The pressures obtained from our simulations at $T = 1000$ and 4000 K and $\rho = 2.2 \text{ g/cm}^3$ (24.7 and ~ 35 GPa) match the reported QM results (25 and 35 GPa). Note that while *ab initio* data on nitromethane has been used to develop ReaxFF (chemical reactions and vibrational properties), none of the QM MD results in ref 4 were included in any way into the ReaxFF parametrization.

Reference 4 used density functional theory with ultrasoft pseudopotentials, a plane waves basis set, and the spin-polarized generalized gradient approximation of Perdew and Wang to describe exchange and correlation. This level of DFT is generally very accurate providing an excellent validation of ReaxFF which has been parametrized against similar quality DFT data (no pseudopotential with the B3LYP flavor of DFT including the Becke GGA exchange functional with the LYP correlational functional and some exact exchange).

These results indicate that ReaxFF accurately describes complex chemical processes in CHNO systems including multi-molecular reactions, ionic reactions, and mechanical properties at extreme conditions. They are similar to results from another set of recently reported ReaxFF simulations on thermal decomposition of liquid NM.³¹ However, our results include, in addition, simulations on crystalline systems and a much more detailed analysis of the chemistry. This detailed and direct validation of the accuracy of the ReaxFF description of the interatomic forces is important since it indicates that we can use ReaxFF for much larger systems and longer times for which the QM MD is currently impractical. This also suggests that the functional forms in ReaxFF, including the description of charge transfer and of bond orders, capture the physics responsible for the chemistry. In addition it supports the value of using an extensive training set containing over 1515 separate reactions and equilibrium molecules designed to characterize atomic interactions under various environments [likely and unlikely (high energy)], including over 50 molecules describing nitromethane and its reactions with water and NH_3 . The training set contains bond dissociation and compression curves of all possible bonds, angles, and torsion bending for all cases, vibrational properties, and equation of state data of crystals.³²

■ CONCLUSIONS

We used ReaxFF with MD to study the thermal decomposition of crystalline and liquid nitromethane at high temperatures (2000–3000 K) and high density ($\rho = 1.97 \text{ g/cm}^3$). At the highest temperature ($T = 3000$ K) the first chemical reaction is

an intermolecular proton transfer process leading to CH_2NO_2 and CH_3NOOH . At lower temperatures ($T = 2000\text{ K}$ and $T = 2500\text{ K}$) the first reaction is often an isomerization leading to CH_3ONO . We also find at very short times an internal proton transfer isomerization reaction leading to aci-nitromethane (CH_2NOOH). Crystalline and liquid samples exhibit the same overall chemistry. The main decomposition product is H_2O ; we find $\sim 0.8\text{ H}_2\text{O}$ molecules per original nitromethane in all cases studied. Other products we observe are CO_2 , NH_3 , and N_2 . Finally, while the time scales we obtain from the ReaxFF simulations are similar to previously published rates in simulations using quantum-mechanics-based simulations, the reaction zone in NM involves longer time scales of a few nanoseconds, see ref 30 for a compilation of data. We believe an important contributing factor for this discrepancy is that during detonation the reactive material expands as the reaction proceeds in the reaction zone leading to slower chemistry.

AUTHOR INFORMATION

Corresponding Author

*E-mail: strachan@purdue.edu.

ACKNOWLEDGMENT

S.H. would like to thank the Seaborg Institute for a summer fellowship, Jason Keith for preparation of the ReaxFF training set, and P.W.K. Rothmund for help in formatting the manuscript. Work at Los Alamos was supported by the ASC Materials and Physics modeling project and DARPA (program manager Carey Schwatz). Work at Caltech is supported by ONR (N00014-09-1-0634, program manager Cliff Bedford), LANL (65287-001-08, program manager Ed Kober), and DARPA (program manager Carey Schwatz).

REFERENCES

- (1) Chakraborty, D.; Muller, R. P.; Dasgupta, S.; Goddard, W. A., III. *J. Phys. Chem. A* **2000**, *104*, 2261.
- (2) Chakraborty, D.; Muller, R. P.; Dasgupta, S.; Goddard, W. A., III. *J. Comput.-Aided Mater. Des.* **2001**, *8*, 203.
- (3) Jacob, T. *Fuel Cells* **2006**, *6*, 159.
- (4) Manaa, M. R.; Reed, E. J.; Fried, L. E.; Galli, G.; Gygi, F. *J. Chem. Phys.* **2004**, *120*, 10146.
- (5) Bickham, S. R.; Kress, J. D.; Collins, L. A. *J. Chem. Phys.* **2000**, *112*, 9695.
- (6) Manaa, M. R.; Fried, L. E.; Melius, C. F.; Elstner, M.; Frauenheim, T. *J. Phys. Chem. A* **2002**, *106*, 9024.
- (7) Reed, E. J.; Fried, L. E.; Joannopoulos, J. D. *Phys. Rev. Lett.* **2003**, *90*, 235503.
- (8) Reed, E. J.; Manaa, M. R.; Fried, L. E.; Glaesemann, K. R.; Joannopoulos, J. D. *Nat. Phys.* **2008**, *4*, 72.
- (9) van Duin, A. C. T.; Dasgupta, S.; Lorant, F.; Goddard, W. A., III. *J. Phys. Chem. A* **2001**, *105*, 9396.
- (10) Zhang, Q.; Cagin, T.; van Duin, A. C. T.; Goddard, W. A., III. *Phys. Rev. B* **2004**, *69*, 045423.
- (11) van Duin, A. C. T.; Strachan, A.; Stewman, S.; Zhang, Q.; Xu, X.; Goddard, W. A., III. *J. Phys. Chem. A* **2003**, *107*, 3803.
- (12) Strachan, A.; van Duin, A. C. T.; Chakraborty, D.; Dasgupta, S.; Goddard, W. A., III. *Phys. Rev. Lett.* **2003**, *91*, 098301.
- (13) Strachan, A.; Kober, E. M.; van Duin, A. C. T.; Oxgaard, J.; Goddard, W. A., III. *J. Chem. Phys.* **2005**, *122*, 054502.
- (14) Blais, N. C.; Engelke, R.; Sheffield, S. A. *J. Phys. Chem. A* **1997**, *101*, 8285.

- (15) Engelke, R.; Earl, W. L.; Rohlfing, C. M. *Int. J. Chem. Kinet.* **1986**, *18*, 1205.
- (16) Citroni, M.; Bini, R.; Pagliai, M.; Cardini, G.; Schettino, V. *J. Phys. Chem. B* **2010**, *114*, 9420–9428.
- (17) Piermarini, G. J.; Block, S.; Miller, P. J. *J. Phys. Chem.* **1989**, *93*, 457.
- (18) Engelke, R.; Earl, W. L.; Rohlfing, C. M. *J. Phys. Chem.* **1986**, *90*, 545.
- (19) Brenner, D. W.; Shenderova, O. A.; Harrison, J. A.; Stuart, S. J.; Ni, B.; Sinnott, S. B. *J. Phys.: Condens. Matter* **2002**, *14*, 783.
- (20) Elert, M. L.; Deaven, D. M.; Brenner, D. W.; White, C. T. *Phys. Rev. B* **1989**, *39*, 1453.
- (21) Brenner, D. W.; Robertson, D. H.; Elert, M. L.; White, C. T. *Phys. Rev. Lett.* **1993**, *70*, 2174.
- (22) Mintmire, J. W.; Barrett, J. J. C.; Robertson, D. H.; White, C. T. *Chem. Phys. Rep.* **1998**, *17*, 37.
- (23) Holian, B. L.; Germann, T. C.; Maillet, J. B.; White, C. T. *Phys. Rev. Lett.* **2002**, *89*, 285501.
- (24) White, C. T.; Robertson, D. H.; Swanson, D. R.; Elert, M. L. *AIP Conf. Proc.* **2000**, *505*, 377.
- (25) Rice, B. M.; Mattson, W.; Trevino, S. F. *Phys. Rev. E* **1998**, *57*, 5106.
- (26) Zhang, L.; van Duin, A. C. T.; Zybin, S. V.; Goddard, W. A., III. *J. Phys. Chem. A* **2009**, *113*, 10770.
- (27) Mayo, S. L.; Olafson, B. D.; Goddard, W. A., III. *J. Phys. Chem.* **1990**, *94*, 8897.
- (28) Nguyen, M. T.; Le, H. T.; Hajato, B.; Veszpremi, T.; Lin, M. C. *J. Phys. Chem. A* **2003**, *107*, 4286.
- (29) Zhu, R. S.; Lin, M. C. *Chem. Phys. Lett.* **2009**, *478*, 11–16.
- (30) Tarver, M. C. *Shock Compression Condens. Matter* **2006**, *845*, 1026–1029.
- (31) Hervout, A.; Desbiens, N.; Bourasseau, E.; Maillet, J. B. *J. Phys. Chem. B* **2008**, *112*, 5070.
- (32) Zhang, L.; van Duin, A. C. T.; Zybin, S. V.; Goddard, W. A., III. *J. Phys. Chem. B* **2009**, *113*, 10770.